World Academy of Science, Engineering and Technology
International Journal of Energy and Power Engineering
Vol:11, No:7, 2017

Applying Different Working Fluids in a Combined Power and Ejector Refrigeration Cycle with Low Temperature Heat Sources

Samad Jafarmadar, Amin Habibzadeh

***Abstract*—**A power and cooling cycle, which combines the organic Rankine cycle and the ejector refrigeration cycle supplied by waste heat energy sources, is discussed in this paper. 13 working fluids including wet, dry, and isentropic fluids are studied in order to find their performances on the combined cycle. Various operating conditions' effects on the proposed cycle are examined by fixing power/refrigeration ratio. According to the results, dry and isentropic fluids have better performance compared with wet fluids.

***Keywords*—**Combined power and refrigeration cycle, low temperature heat sources, organic rankine cycle, working fluids.

I. Introduction

IN recent years, scientist and engineers have tried to find more efficient power systems to reduce environmental problems such as atmospheric pollution, acid precipitation, ozone depletion, and global warming. Low temperature heat sources, such as waste heat and renewable energies (geothermal energy and solar energy) exist in the considerable quantities. Due to these reasons, exploring combined power and refrigeration cycles which use such low-grade heat sources has gained more and more attention.

A novel combined power and ejector refrigeration cycle was proposed by Dai et al. [1]. The cycle combined the Rankine cycle and the ejector refrigeration cycle by adding a turbine between the boiler and the ejector. The vapor from the boiler could be expanded through the turbine to generate power, and the turbine exhaust can drive the ejector.

Wang et al. [2] studied this cycle with R123. According to the results, the biggest exergy destruction occurs in the heat recovery vapor generator; it can be reduced by increasing the area of heat transfer and the coefficient of heat transfer in the HRVG. For more performed investigation related to ORCs, see [3]-[7].

In the present study, a combined power and refrigeration cycle is proposed to produce both power and refrigeration by utilizing different working fluids and a low-grade heat source. This cycle combines the ORC and the ejector refrigeration cycle. First and second law analysis is conducted to compare different working fluids and different working conditions.

Samad Jafarmaadar is with the Mechanical Engineering Department, Urmia University, Urmia, Iran (e-mail: s.jafarmadar@ urmia.ac.ir).

Amin Habibzadeh is with the Mechanical Engineering Department, Urmia University, Urmia, Iran (corresponding author, e-mail: a.habibzadeh@urmia.ac.ir).

II. Cycle Operation and Assumptions

In this study, the waste heat is used as the heat source to simulate the combined power and ejector refrigeration cycle shown in Fig. 1. To simplify the modeling of the combined cycle, the following assumptions are made:

(1) Steady state condition in the system is considered.
(2) The friction losses and kinetic and potential energies are neglected.
(3) Adiabatic conditions have been assumed for evaporator, condenser, vapor generator, ejector, and turbine.
(4) The isenthalpic process has been considered for the expansion valve.
(5) The evaporator outlet is saturated vapor.
(6) The condenser outlet is saturated liquid.
(7) A temperature difference of 10 K is assumed between state 2 and state 9.
(8) A temperature difference of 10 K is assumed between state 4 and state 16.
(9) A temperature difference of 10 K is assumed between state 13 and state 14.

The base case conditions for the simulation of the combined cycle are summarized in Table I.

TABLE I
Physical, Safety and Environmental Data for Analyzed Fluids

Environment temperature (K)	298.15
Environment pressure (kPa)	101.325
Turbine inlet pressure (MPa)	0.6
Turbine inlet temperature (K)	373.15
Turbine extraction pressure (MPa)	0.2
Extraction ratio	0.35
Turbine isentropic efficiency (%)	85
Pump inlet temperature (K)	293.15
Pump isentropic efficiency (%)	80
Evaporator temperature (K)	263.15
Heat source mass rate (kg/s)	75
Power refrigeration ratio	2.5
Cooling water mass rate (kg/s)	20
Cooling water inlet temperature (K)	288.15

III. Choice of Working Fluids

One of the main concerns for choosing a working fluid is its environmental effects. Ozone depletion potential (ODP), global warming potential (GWP), and atmospheric lifetime (ALT) are the three important factors that should be regarded. Fortunately, most working fluids used in the ORC cycle can be used in the ejector refrigeration cycle.

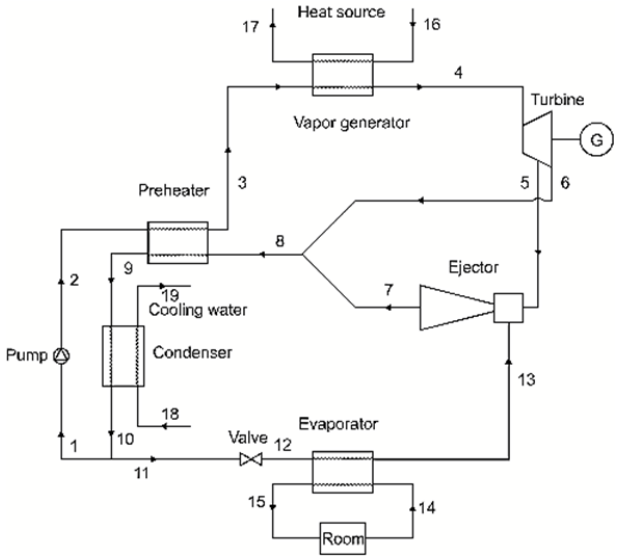

Fig. 1 Schematic diagram of the combined power and ejector refrigeration cycle

IV. Thermodynamic Analysis

A. Energy Analysis

$$\dot{Q}_{con} = \dot{m}_9(h_9 - h_{10}) \tag{1}$$

$$\dot{Q}_{eva} = \dot{m}_{12}(h_{13} - h_{12}) \tag{2}$$

$$\dot{Q}_{ph} = \dot{m}_1(h_3 - h_2) \tag{3}$$

$$-\dot{W}_p = \dot{m}_1(h_2 - h_1) \tag{4}$$

$$\eta_p = \frac{h_{2s} - h_1}{h_2 - h_1} \tag{5}$$

$$\dot{W}_t = \dot{m}_4(h_4 - h_5) + (\dot{m}_4 - \dot{m}_5)(h_5 - h_6) \tag{6}$$

$$\dot{m}_5 h_5 + \dot{m}_{13} h_{13} = \dot{m}_7 h_7 \tag{7}$$

$$\eta_t = \frac{h_4 - h_6}{h_4 - h_{6s}} \tag{8}$$

$$\dot{W}_t = \dot{m}_4(h_4 - h_5) + (\dot{m}_4 - \dot{m}_5)(h_5 - h_6) \tag{9}$$

$$R_{extr} = \frac{\dot{m}_5}{\dot{m}_4} \tag{10}$$

$$\beta = \frac{P_4}{P_5} \tag{11}$$

$$\dot{Q}_{vg} = \dot{m}_3(h_4 - h_3) \tag{12}$$

$$\dot{W}_{net} = \dot{W}_t + \dot{W}_p \tag{13}$$

B. Exergy Analysis

Energy efficiencies provide neither information of how nearly the performance of a system approaches ideality nor the reversibility aspects of the thermodynamic processes. To determine more meaningful efficiencies, a quantity which provides a measure of an approach to an ideal is required. Thus, exergy efficiency must be introduced. Exergy destruction equations for condenser, ejector, evaporator, preheater, pump, expansion valve, turbine and vapor generator are as follows:

$$\dot{I}_{con} = \dot{E}_9 + \dot{E}_{18} - \dot{E}_{10} - \dot{E}_{19} \tag{14}$$

$$\dot{I}_{eje} = \dot{E}_5 + \dot{E}_{13} - \dot{E}_7 \tag{15}$$

$$\dot{I}_{eva} = \dot{E}_{12} + \dot{E}_{ref} - \dot{E}_{13} \tag{16}$$

$$\dot{I}_{ph} = \dot{E}_2 + \dot{E}_8 - \dot{E}_3 - \dot{E}_9 \tag{17}$$

$$\dot{I}_p = -\dot{W}_p + \dot{E}_1 - \dot{E}_2 \tag{18}$$

$$\dot{I}_{exv} = \dot{E}_{11} - \dot{E}_{12} \tag{19}$$

$$\dot{I}_t = \dot{E}_4 - \dot{E}_5 - \dot{E}_6 - \dot{W}_t \tag{20}$$

$$\dot{I}_{vg} = \dot{E}_3 + \dot{E}_{16} - \dot{E}_4 - \dot{E}_{17} \tag{21}$$

$$\dot{I}_{tot} = \dot{I}_{con} + \dot{I}_{eje} + \dot{I}_{eva} + \dot{I}_{ph} + \dot{I}_p + \dot{I}_{exv} + \dot{I}_t + \dot{I}_{vg} \tag{22}$$

C. Efficiency

$$\eta_{th} = \frac{\dot{W}_{net} + \dot{Q}_{eva}}{\dot{Q}_{vg}} \tag{23}$$

$$\eta_{exe} = \frac{\dot{W}_{net} + \dot{E}_{ref}}{\dot{E}_{in}} \tag{24}$$

D. Entrainment Ratio

The performance of an ejector is evaluated by its entrainment ratio, which is defined as the mass flow rate ratio of the secondary fluid to that of the primary fluid:

$$\mu = \frac{\dot{m}_{sf}}{\dot{m}_{pf}} \tag{25}$$

V. Validation

Based on the above analysis, a simulation program using EES software [8] for the combined ORC and ejector

refrigeration cycle was developed. The obtained solution is validated with the results of Dai et al. [1] in which R123 was selected as the working fluid which shows a very good agreement.

VI. Results and Discussion

The detailed data of the analyzed cycles for 13 different working fluids are listed in Table III.

A. Exergy Analysis Effects of Evaporator Temperature $(T_{12} = T_{13})$

Fig. 2 shows that the exergy efficiency decreases with the increase in the evaporator temperature. The reduction of the refrigeration output exergy and the entrainment ratio of the ejector are the main reasons of the exergy decrease.

The results shown in Fig. 3 indicate that the entrainment ratio of the cycle for all of the working fluids decreases with increasing evaporator temperature.

B. Effects of Turbine Inlet Temperature (T_4)

It is found from Fig. 4 that the exergy efficiency of the cycle increases with increasing turbine inlet temperature. As the power/refrigeration ratio is kept constant, turbine inlet temperature will affect the ejector entrainment ratio which leads to the increase of the refrigeration output exergy.

As shown in Fig. 5, the total exergy destruction in the cycle increases monotonically with the turbine inlet temperature.

According to Fig. 6, when the turbine inlet temperature goes up, also the thermal efficiency rises. As the inlet temperature increases, the turbine power, the net power output, and the entrainment ratio rise correspondingly.

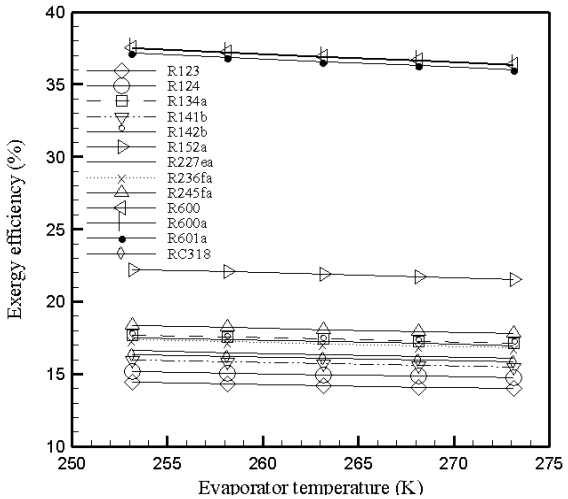

Fig. 2 Effect of the evaporator temperature on the exergy efficiency

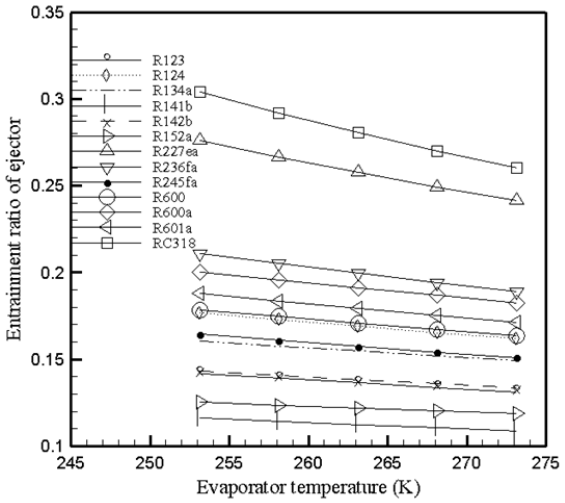

Fig. 3 Effect of the evaporator temperature on the entrainment ratio of ejector

TABLE II
Validation of the Numerical Model with the Previously Published Data

Parameter	This work	Dai et al. [1]
Generating temperature (K)	413	413
Condensing temperature (K)	293	293
Evaporating temperature (K)	263	263
Heat input (kJ/kg)	1263	1246.96
Entrainment ratio	0.396	0.389
Pump work (kJ/kg)	3.45	3.45
Turbine work (kJ/kg)	115.8	114.14
Net work (kJ/kg)	112.35	110.69
Refrigeration capacity (kJ/kg)	61.61	60.44
Thermal efficiency (%)	13.77	13.72
Exergy efficiency (%)	22.53	22.2

TABLE III
COMPARISON OF THE COMBINED POWER AND REFRIGERATION CYCLE WITH 13 DIFFERENT WORKING FLUIDS

Element	Unit	R123	R124	R134a	R141b	R142b	R152a	R227ea
μ	-	0.1364	0.1692	0.1549	0.1124	0.1384	0.1219	0.2576
$\dot{m}$	kgs^{-1}	2.049	4.075	6.507	1.678	3.133	4.587	6.41
$\dot{I}_{con}$	kW	6.506	10.02	14.5	6.722	9.632	14.66	12.23
$\dot{I}_{eje}$	kW	8.495	14.95	19.37	10.8	12.55	18.8	23.25
$\dot{I}_{eva}$	kW	0.2373	0.3796	0.6818	0.07173	0.4053	0.6525	0.6363
$\dot{I}_{exv}$	kW	0.2648	0.36	0.4311	0.2262	0.3447	0.4292	0.5734
$\dot{I}_{p}$	kW	0.1821	0.202	0.03708	0.1805	0.2182	0.1087	0.2445
$\dot{I}_{ph}$	kW	1.415	9.043	41.92	1.356	5.888	28.64	23.33
$\dot{I}_{t}$	kW	9.857	9.857	11.29	10.34	11.34	14.24	10.79
$\dot{I}_{vg}$	kW	17.57	38.86	94.8	14.43	76.51	97.4	89.11
$\dot{Q}_{eva}$	kW	21.22	22.34	25.59	23.44	25.71	32.27	24.47
$\dot{Q}_{in}$	kW	426.6	701.1	1318	458.7	740.4	1448	855.6
$\dot{W}_{t}$	kW	53.04	55.86	63.98	58.6	64.27	80.69	61.17
$\dot{W}_{p}$	kW	0.9105	1.01	0.1854	0.9027	1.091	0.5436	1.223
$\dot{W}_{net}$	kW	52.13	54.85	63.8	57.7	63.18	80.14	59.95
Refrigeration exergy	kW	1.942	2.342	2.374	2.145	2.353	2.954	2.343
η_{th}	$\%$	17.19	11.01	6.781	17.69	12.01	7.762	9.866
η_{exe}	$\%$	14.23	14.97	17.41	15.75	17.25	21.87	16.37
μ	-	**R236fa**	**R245fa**	**R600**	**R600a**	**R601a**	**RC318**	
$\dot{m}$	kgs^{-1}	0.1995	0.1574	0.1708	0.191	0.1792	0.2805	
$\dot{I}_{con}$	kW	4.04	2.716	3.151	4.05	2.498	5.473	
$\dot{I}_{eje}$	kW	9.921	8.698	14.34	15.09	12.65	9.982	
$\dot{I}_{eva}$	kW	5.811	5.372	8.091	10.41	22.07	8.591	
$\dot{I}_{exv}$	kW	0.9225	0.4603	2.183	0.8372	0.498	0.6151	
$\dot{I}_{p}$	kW	0.4726	0.3761	0.7698	0.9279	0.7215	0.5796	
$\dot{I}_{ph}$	kW	0.272	0.2398	0.5336	0.5406	0.5275	0.3013	
$\dot{I}_{t}$	kW	8.215	3.874	10.14	18.35	4.992	12.34	
$\dot{I}_{vg}$	kW	11.29	11.9	24.3	24.32	24.1	10.67	
$\dot{Q}_{eva}$	kW	62.28	37.08	51.75	77.96	46.53	62.88	
$\dot{Q}_{in}$	kW	25.46	26.97	55.21	55.12	54.63	24.18	
$\dot{W}_{t}$	kW	707.9	622.1	1357	1551	1059	694.9	
$\dot{W}_{p}$	kW	64	67.41	138	137.8	136.6	60.44	
$\dot{W}_{net}$	kW	1.36	1.199	2.668	2.703	2.638	1.507	
Refrigeration exergy	kW	62.64	66.22	135.4	135.1	133.9	58.94	
η_{th}	$\%$	2.33	2.468	5.053	5.045	5	2.213	
η_{exe}	$\%$	12.46	14.98	14.05	12.26	17.8	11.96	
μ	-	17.1	18.07	36.95	36.88	36.57	16.09	

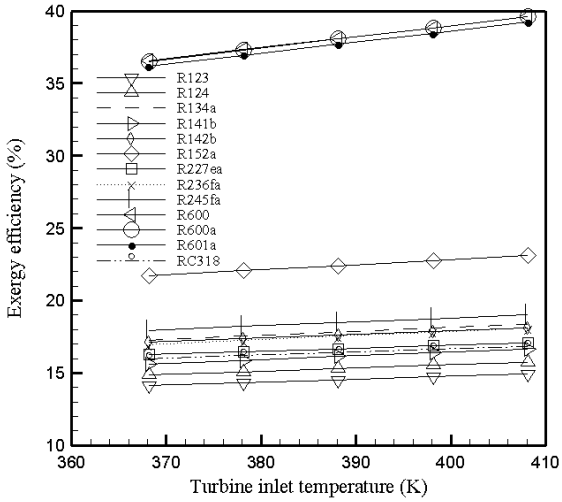

Fig. 4 Effect of the turbine inlet temperature on the exergy efficiency

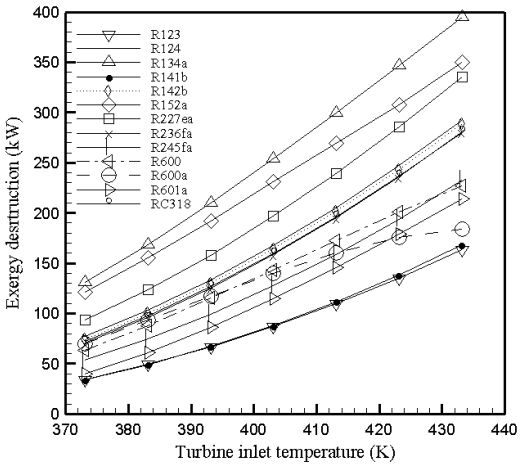

Fig. 5 Effect of the turbine inlet temperature on the total exergy destruction

C. Effects of Heat Source Temperature (T_{16})

Fig. 7 shows that increase in the heat source fluid temperature leads to the increase in the exergy efficiency. Since the mass flow rate of the turbine and the entrainment ratio of the ejector rise as the vapor generator temperature goes up, the turbine work output and the cooling capacity increase similarly.

D. Effects of Expansion Ratio

From Fig. 8, it is apparent that when the expansion ratio of the turbine increases from 2 to 6, the thermal efficiency rises for all of the working fluids. The reason for this is that increasing expansion ratio leads to a decrease in the temperature and pressure of the primary flow entering the ejector.

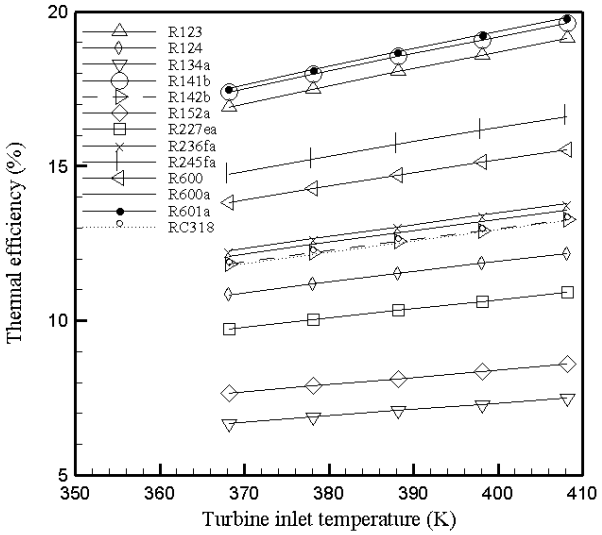

Fig. 6 Effect of the turbine inlet temperature on the thermal efficiency

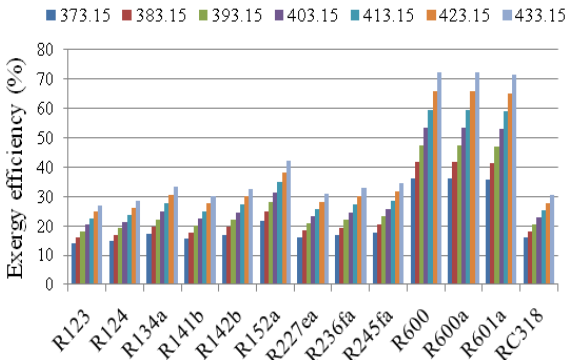

Fig. 7 Effect of the heat source temperature on the exergy efficiency

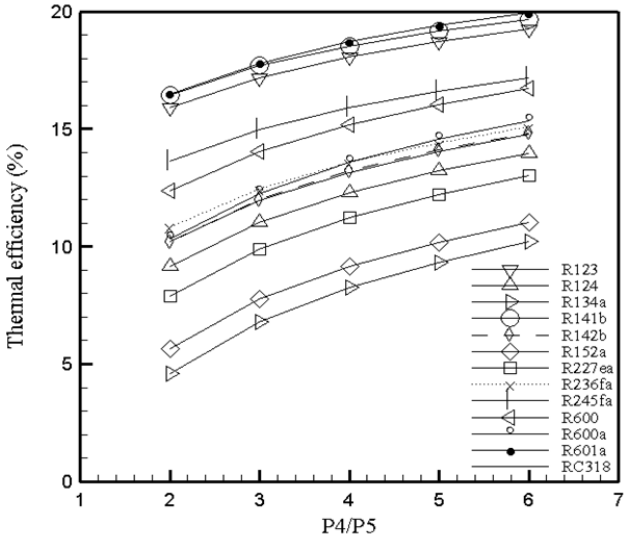

Fig. 8 Effect of the expansion ratio on the thermal efficiency

VII. . Conclusions

The main conclusions from this study are as follows:

(1) According to the findings, dry and isentropic fluids

showed better results compared with the wet ones.

(2) Increasing evaporator temperature leads to the decrease in the exergy efficiency, but exergy efficiency increases when turbine inlet temperature decreases and heat source temperature rises.

(3) When the turbine inlet temperature and turbine expansion ratio goes up, the thermal efficiency of the cycle increases.

(4) Increasing evaporator temperature leads to the decrease in the entrainment ratio of the ejector.

(5) From the exergy efficiency and environmental friendly point of view, R600 and R600a are the most suitable working fluids for the proposed combined cycle among the different working fluids studied in this paper.

REFERENCES

[1] Y. Dai, J. Wang, and L. Gao, "Exergy analysis, parametric analysis and optimization for a novel combined power and ejector refrigeration cycle," J. Appl Therm Eng, 29, 1983–1990, 2009.

[2] J. Wang, Y. Dai, and Z. Sun, "A theoretical study on a novel combined power and ejector refrigeration cycle," Int. J. Ref. 32, 1186-1194, 2009.

[3] M. M. Rashidi, O. Anwar Bég, A. Basiri Parsa, and F. Nazari, "Analysis and optimization of a transcritical power cycle with regenerator using artificial neural networks and genetic algorithms," J *Proceedings of the Institution of Mechanical Engineers, Part A: Journal of Power and Energy*. 225**,** 701-717, 2011.

[4] E. Cayer, N. Galanis, M. Desilets, H. Nesreddine, and P. Roy, "Analysis of a carbon dioxide transcritical power cycle using a low temperature source," 2009 J Applied Energy. 86, 1055–1063, 2009.

[5] B. L. Lostec, J. Millette and N. Galanis, "Finite time thermodynamics study and exergetic analysis of ammoniaewater absorption systems," International Journal of Thermal Sciences. 49, 1264-1276, 2010.

[6] E. Cayer, N. Galanis, and H. Nesreddine, "'Parametric study and optimization of a transcritical power cycle using a low temperature source," J Applied Energy. 87, 1349–1357, 2010.

[7] P. Roy, M. De´ silets, N. Galanis, H. Nesreddine, and E. Cayer, "Thermodynamic analysis of a power cycle using a low-temperature source and a binary NH3–H2O mixture as working fluid," 2010 International Journal of Thermal Sciences. 49, 48–58, 2010.

[8] S. A. Klein, Engineering equation solver version 7.171 (McGraw Hill), 2004.